USP7 Inhibition Promotes Mesenchymal Stem cell-Macrophage Crosstalk in Age-related Osteoporosis via Efferocytosis and Senolysis

Authors: Feng Zhou[1,2], Zhanqi Wang[1,2], Haiyun Li[1,2], Dongyang Wang[1,2], Zhongyu Wu[1,2], Fuwei Bai[1,2], Qingyi Wang[1], Wenxin Luo[1], Guorui Zhang[1], Yi Xiong[1,2,3], Yingying Wu[1,2]*

Affiliations:

[1]State Key Laboratory of Oral Diseases, National Clinical Research Center for Oral Diseases, West China Hospital of Stomatology, Sichuan University; Wuhou district, Chengdu, China

[2]Department of Oral Implantology, West China Hospital of Stomatology, Sichuan University; Wuhou district, Chengdu, China

[3]Lead contact

*Corresponding author. Email: yywdentist@163.com.

Summary:

The interaction between bone mesenchymal stem cells (BMSCs) and macrophages in osteoporosis has gained increasing attention. Aged BMSCs exhibit a senescence-associated secretory phenotype (SASP), which contributes to the inflammatory microenvironment with macrophage inflammaging. USP7, as a key deubiquitinase regulating cellular senescence and inflammation, has been found to promote senolysis when inhibited. We found that USP7 inhibition induced senolysis and osteogenic differentiation in aged BMSCs. For senescent BMDMs, USP7 inhibition suppressed inflammaging and enhanced efferocytosis through EPSIN1/LRP1 pathway, enabling them to efficiently clear apoptotic senescent cells caused by USP7 inhibition. In the femurs and vertebrae of aged mice, it was discovered that USP7 inhibition could rescue bone loss, which may be associated with improved macrophage efferocytosis. This study highlights the potential of USP7 inhibition in promoting senolysis in aged BMSCs and enhancing efferocytosis capacity of senescent BMDMs, which exerts a synergistic therapeutic effect by inducing senescent cell apoptosis and immune clearance.

Key words: USP7, cell communication, osteoimmunology, efferocytosis, aging, osteoporosis

Graphic Abstract:

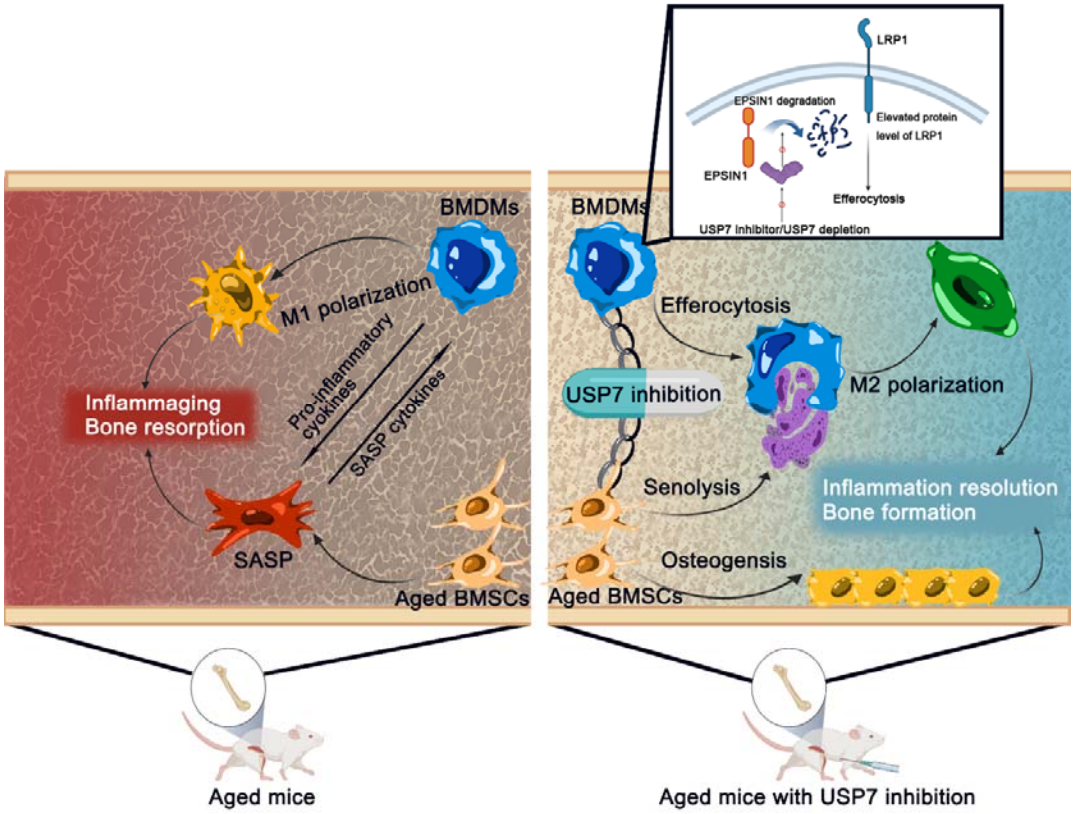

INTRODUCTION

Nowadays, the pace of population aging is intensifying in major countries worldwide. Elderly people typically experience a decrease in bone mineral density and an increased risk of fractures, which is defined as osteoporosis (*1*). In addressing this public health problem, a multitude of therapies and medications have been proposed, such as bisphosphonates, denosumab, teriparatide, selective estrogen receptor modulators (SERMs) and calcium/vitamin D supplementation (*2*, *3*). Among them, bisphosphonates and denosumab, which inhibit bone resorption, have been found to potentially interfere with osteoblast function, leading to bisphosphonate-related osteonecrosis of the jaw (BRONJ) (*4*, *5*). Another commonly used drug, vitamin D, has been found to have immunomodulatory effects on the inflammatory microenvironment (*6*). Therefore, it could become a new focus in drug development that involves treating the interactions between bone cells and immune cells.

In recent years, there has been increasing attention on the interaction between bone cells and immune cells in osteoporosis, referred to as immunoporosis (*7*). Immunoporosis refers to that both the innate immune system and adaptive immune system can intervene in osteoclastogenesis, osteoblast differentiation, and angiogenesis processes, which affects the onset and progression of osteoporosis (*8*, *9*). In this situation, the innate immune system plays a major role through pathways involving pathogen-associated molecular patterns (PAMPs), damage-associated molecular patterns (DAMPs), and cellular stress (*2*). Numerous studies have revealed that overactive innate immune system

in aged individuals can generate a chronic inflammatory microenvironment, which is called inflammaging and contributes to osteoporosis (*10*). Therefore, the functional changes and interaction patterns between macrophages and bone mesenchymal stem cells (BMSCs) in the aging environment can have a significant impact on the progression and treatment of osteoporosis.

Following this line of thought, the ubiquitin-proteasome system (UPS) is poised to become a key target for improving the aged BMSCs-macrophages crosstalk. UPS is the primary protein degradation system within eukaryotic cells, serving various functions such as clearing misfolded proteins, regulating cellular stress and signaling pathways, and controlling DNA damage repair (*11*). In the UPS system, ubiquitin (Ub) serves as tags to mark substrate proteins through E3 ligases. Subsequently, these substrate proteins are recognized and degraded by the 26S proteasome (*12*). Simultaneously, this process is intricately regulated by the deubiquitination system. Peptidases, termed deubiquitinating enzymes (DUBs), can cleave the ubiquitin chains from substrate proteins, thereby sparing them from degradation (*13*). DUBs can be broadly categorized into six families: Ub C-terminal hydro-lases (UCHs), Ub-specific proteases (USPs), Machado-Josephindomain proteases (MJDs), ovarian tumor proteases (OTUs),motif interacting with Ub-containing novel DUB family (MINDY),and zinc-finger-containing Ub peptidase (ZUP1) (*14*).

Among many family members of DUBs, USP7 has been recently discovered to have a role in regulating the aging process. He et al. found that inhibiting USP7 could selectively induce apoptosis in ionizing radiation-induced senescent fibroblasts, and the USP7 inhibitor P5091 could clear senescent cells induced by doxorubicin in mice (*15*). This suggests that USP7 inhibition may be a potential approach for improving age-related diseases via senolysis. Senolysis and senotherapy refer to the selective removal of senescent cells without affecting normal cells, which can avoid tissue damage caused by senescent cells producing SASP cytokines like IL-1β and IL-6 (*16*). Therefore, we speculated that USP7 might be an important target for the treatment of age-related osteoporosis.

In this study, we established a BMSCs-macrophage crosstalk model by co-culturing aged BMSCs and bone marrow-derived macrophages (BMDMs). Through USP7 depletion and the use of USP7 inhibitor P5091, we found that USP7 not only selectively eliminated aged BMSCs but also inhibited the inflammaging of BMDMs. Furthermore, we have discovered, for the first time through RNA-Seq, that USP7 inhibition could enhance the efferocytosis capacity of senescent BMDMs, enabling them to efficiently clear apoptotic cells and undergo M2 polarization. Moreover, these results have been further validated in mice through systemic injection of P5091.USP7 inhibition, therefore, results in synergistic effects of enhanced BMDMs efferocytosis and increased apoptosis levels in BMSCs, which together play a "kill and bury" role to alleviate osteoporosis.

USP7 inhibition ameliorates inflammaging of senescent macrophages

To assess the impact of USP7 depletion on senescent macrophages, the following experimental procedures were conducted. Initially, yound and aged BMSCs were isolated from 3-month-old and 20-month-old mice. Then the conditioned media (CM) derived

from young BMSCs and aged BMSCs was designated as control CM and senescent CM, respectively. These CMs were subsequently utilized to culture BMDMs. BMDMs cultured with control CM were employed as the control group (CON) to simulate normal BMDMs, whereas BMDMs cultured with senescent CM were represented as senescent group (SEN) (Fig. 1A).

To gain further insights into the mechanistic role of USP7 in senescent BMDMs, shRNA targeting *Usp7* was transfected into normal and senescent BMDMs to deplete USP7 expression (Fig. S1A-B). mRNA-Seq analysis was performed on senescent BMDMs, revealing a notable downregulation of genes associated with the innate immune response pathway and NLRP3 pathway in USP7-depleted BMDMs (Fig. 1B). Gene set enrichment analysis (GSEA) supported these findings, demonstrating a decreased activity of the innate immune response and NLRP3 pathway in USP7-depleted senescent BMDMs (Fig. 1C-D). Results obtained from qPCR validated the results of GSEA, demonstrating significantly upregulated mRNA expression levels of *Il-6*, *Il-1b*, and *Tnf-a* in senescent BMDMs compared to normal BMDMs. However, USP7 depletion suppressed the expression of these genes in senescent BMDMs (Fig. 1E). Furthermore, NLRP3 inflammasome signaling pathway was studied using Western blot, which indicated its downregulation upon USP7 depletion in senescent BMDMs (Fig. 1F-G). Additionally, the secretion of IL-1β and IL-6 in the culture media of senescent BMDMs was reduced following USP7 depletion (Fig. 1H). Subsequently, flow cytometry was applied to investigate the effect of USP7 on macrophage polarization. M2/M1 ratio was significantly increased in senescent BMDMs upon USP7 depletion (Fig. 1I).

Moreover, we conducted further investigations into the pharmacological effects targeting USP7. P5091, a selective inhibitor targeting USP7 widely used in various disease models, was employed. Based on CCK8 assays, the optimal concentration for treating BMDMs and BMSCs was determined to be 5μM (Fig. S1C). Although P5091 had minimal effects on normal BMDMs, it significantly inhibited the mRNA expression of *Il-6*, *Il-1b*, and *Tnf-a* in senescent BMDMs (Fig. S1D). Additionally, P5091 suppressed the secretion of IL-1β and IL-6 in the culture media of senescent BMDMs (Fig. S1E). Western blot analysis further indicated that P5091 inhibited the NLRP3 pathway in senescent BMDMs without affecting the protein levels of NLRP3 and cleaved IL-1β in normal BMDMs (Fig S1F-H).

USP7 inhibition enhanced aged BMSCs osteogenesis co-cultured with macrophages

Subsequently, we investigated the influence of senescent BMDMs on BMSCs and the potential of USP7 depletion to promote BMSC osteogenesis. A transwell co-culture model was employed to facilitate this investigation. Initially, the upper chamber was seeded with USP7-depleted and normal BMDMs, while the lower chamber contained young and aged BMSCs, which were used for CCK8 assay, ALP/ARS staining, SA-β-gal staining, qPCR, and Western blot (Fig. 2A). Next, transwell migration assay was conducted, with BMSCs placed in the upper chamber and BMDMs in the lower chamber, to evaluate cell migration (Fig. 2B). Cell proliferation was detected using CCK-8 assay, revealing that USP7-depleted BMDMs significantly enhanced the proliferation of young BMSCs, while exerting limited effects on aged BMSCs (Fig. 2C).

In contrast to the results obtained from the CCK-8 assay, USP7-depleted BMDMs significantly inhibited the migration of young BMSCs compared to normal BMDMs. However, USP7-depleted BMDMs promoted the migration of aged BMSCs when compared to normal BMDMs (Fig. 2D).

Furthermore, the osteogenesis potential of BMSCs was examined using ALP and ARS staining. The co-culture of aged BMSCs with BMDMs resulted in significantly inhibited osteogenesis. In contrast, USP7-depleted BMDMs in the co-culture rescued the impaired osteogenesis (Fig. 2E). Consistent with this, qPCR analysis demonstrated that aged BMSCs co-cultured with BMDMs exhibited inhibited mRNA expression of *Alp*, *Runx2*, and *Col1a1*. However, USP7-depleted BMDMs enhanced the expression of these genes (Fig. 2H). Additionally, Western blot analysis revealed decreased protein levels of ALP, RUNX2, and COL1A1 in aged BMSCs co-cultured with BMDMs, while USP7-depleted BMDMs significantly upregulated their expression (Fig. 2G-H). Moreover, SA-β-gal staining was performed to confirm the senescence status of BMSCs co-cultured with BMDMs. The staining demonstrated significant senescence phenotype in aged BMSCs co-cultured with BMDMs; however, USP7-depleted BMDMs reversed the senescence phenotype in aged BMSCs (Fig. 2I). Moreover, the expression of SASP markers, such as *Il-1b*, *Il-6*, and *p53*, were evaluated using qPCR (Fig. 2J). The results indicated that USP7-depleted BMDMs were capable of reducing the SASP phenotype of aged BMSCs.

Next, in addition to the sole depletion of USP7 in macrophages, we conducted further investigations to examine the effects of USP7 inhibition in the BMDMs-BMSCs interaction system on the biological behavior and osteogenic capacity of BMSCs (Fig.S2A-B). Initially, P5091 significantly promoted BMSCs proliferation in the normal BMDMs-BMSCs system, but it inhibited BMSCs proliferation in the aged BMDMs-BMSCs system (Fig.S2C). Furthermore, P5091 did not inhibit migration capacity of young BMSCs co-cultured with BMDMs when compared to young BMSCs co-cultured with USP7-depleted macrophages. And P5091 also promoted aged BMSCs migration when co-cultured with BMDMs (Fig.S2D). As for osteogenesis potential, ALP and ARS staining showed that P5091 also promoted osteogenesis capacity of aged BMSCs with BMDMs (Fig. S2E). Although mRNA expression of *Alp* and *Col1a1* were upregulated in aged BMSCs with BMDMs under P5091 treatment, that of *Runx2* was not enhanced under P5091 treatment (Fig.S2F). We further evaluated the protein levels of osteogenesis markers and found that P5091 significantly promoted the expression of ALP, RUNX2, and COL1A1 in aged BMSCs co-cultured with BMDMs. In contrast, expression of COL1A1 in young BMSCs were inhibited after P5091 application (Fig.S2G-H). Additionally, we investigated the senescence status of BMSCs and the expression of senescence-associated SASP markers. We observed reduced SA-β-gal staining and lower SASP mRNA expression in aged BMSCs under P5091 treatment (Fig.S2I-J).

By comparing the co-culture systems where USP7 was exclusively depleted in BMDMs, and the co-culture system where both BMDMs and BMSCs were simultaneously treated with P5091, we found differences in the expression of certain osteogenic genes and

proteins, such as mRNA level of *Runx2* and protein level of COL1A1. These findings suggested that USP7 inhibition might have unique effects on young and aged BMSCs themselves concerning their osteogenic potential.

USP7 inhibition promotes osteogenesis of senescent BMSCs via senolysis

Next, we attempted to investigate the effects of USP7 depletion and P5091-mediated USP7 inhibition on BMSCs. Using the shRNA method, we successfully knocked down USP7 expression in BMSCs (Fig. S3A-B). Firstly, through RNA-Seq analysis, GSEA showed that USP7 depletion in aged BMSCs lead to a reduction in the senescence-associated secretory phenotype (SASP), promotion of osteogenic differentiation, and induction of cell apoptosis (Fig. 3A-B). Furthermore, CCK-8 assays revealed that USP7 depletion enhanced cell proliferation of young BMSCs but attenuated the proliferation of aged BMSCs (Fig. 3C). Transwell migration assays also confirmed that USP7 depletion promoted the migration of aged BMSCs (Fig. 3D).

Regarding osteogenic capacity, ALP and ARS staining showed that USP7 depletion weakened the osteogenic potential of young BMSCs, while significantly enhancing the osteogenic capacity of aged BMSCs (Fig. 3E). qPCR analysis revealed an increase in the mRNA expression levels of *Alp, Runx2,* and *Col1a1* upon USP7 depletion in aged BMSCs (Fig. 3F). However, Western blot analysis indicated that USP7 depletion caused a significant reduction in the protein levels of ALP and COL1A1 in young BMSCs, while rescuing these markers in aged BMSCs (Fig. 3G-H).

Subsequently, we explored whether USP7 exhibited senolytic effects. USP7 depletion significantly reduced the number of SA-β-gal-positive cells and the SASP phenotype in aged BMSCs (Fig. 3I-J). Live-dead cell staining also revealed that USP7 depletion promoted cell death specifically in aged BMSCs without affecting young BMSCs (Fig. 3K, M). Flow cytometry results indicated that USP7 depletion had minimal impact on apoptosis levels in young BMSCs, whereas it significantly increased the proportion of apoptotic cells in aged BMSCs (Fig. 3L, N)

In addition to using shRNA, we also employed P5091 to inhibit USP7 in BMSCs. Firstly, in contrast to the specific effects of USP7 shRNA, P5091 significantly inhibited the proliferation of both young and aged BMSCs (Fig. S3C). However, regarding migration capacity, P5091 suppressed the migration activity of young BMSCs but significantly enhanced the migration activity of aged BMSCs (Fig. S3D). In terms of osteogenic capacity, ALP staining results indicated that P5091 had minimal effect on young BMSCs but significantly increased the early osteogenic potential of aged BMSCs. However, ARS staining revealed that USP7 inhibition diminished the mineralization ability of young BMSCs while significantly enhancing the mineralization ability of aged BMSCs (Fig. S3E). Moreover, qPCR experiments demonstrated that USP7 inhibition had little impact on the mRNA levels of *Alp, Runx2*, and *Col1a1* in young BMSCs, but markedly increased the expression of *Alp* in aged BMSCs (Fig. S3F). Next, we assessed the impact of P5091 on the protein levels of ALP, RUNX2, and COL1A1. We observed that P5091 significantly suppressed the expression of osteogenic marker proteins in young BMSCs, while substantially increasing the expression of these proteins in aged BMSCs (Fig. S3G-H).

Furthermore, we investigated the effects of P5091 as a potential senolytic drug. P5091 reduced the number of SA-β-gal-positive cells and suppressed the expression of SASP-related genes (Fig. S3I-J). Similar to the shRNA effect, live-dead cell staining and flow cytometry results indicated that P5091 increased apoptosis levels in aged BMSCs without affecting young BMSCs (Fig. S3K-L).

USP7 inhibition rejuvenates efferocytosis in senescent macrophages partially through upregulating LRP1

After elucidating that USP7 depletion could alleviate inflammaging in senescent BMDMs and promote senolysis in aged BMSCs, we further investigated whether USP7 depletion affects the efferocytosis function of macrophages. Through GSEA, we found that the apoptotic cell clearance pathway was significantly enhanced in USP7-depleted senescent BMDMs (Fig. 4A-B). qPCR showed that key efferocytosis genes, *CD36, Mertk,* and *Lrp1*, were significantly upregulated in USP7-depleted BMDMs. Because researches have found that LRP1 plays a significant role in both bone homeostasis and macrophage efferocytosis, we have focused on investigating the role of LRP1 (*17*). The use of LRP1 inhibitor RAP significantly inhibited the expression of efferocytosis-related genes (Fig. 4C). Subsequently, we labeled Jurkat cells with calcein-AM, giving them green fluorescence, and co-cultured them with BMDMs to evaluate efferocytosis efficiency. The results revealed that the ability of senescent BMDMs to engulf apoptotic cells was significantly reduced, but USP7 depletion significantly enhanced the efferocytosis capacity of senescent BMDMs. However, the use of RAP counteracted the promoting effect of USP7 depletion on efferocytosis (Fig. 4D). Furthermore, we quantitatively measured efferocytosis efficiency through flow cytometry. Using DiIC18(5)-DS to label apoptotic Jurkat cell membranes, we calculated the ratio of DiIC18(5)-DS and F4/80 double-positive cells to determine efferocytosis efficiency. The results demonstrated that USP7 depletion significantly increased the efferocytosis efficiency of senescent BMDMs, while RAP weakened the promoting effect of USP7 depletion (Fig. 4E).

Considering that efferocytosis plays a crucial role in promoting M2 polarization of macrophages, we investigated the effects of USP7 depletion on M2 polarization and osteogenic regulation in BMDMs after efferocytosis. Flow cytometry analysis of BMDMs co-cultured with apoptotic cells revealed that the proportion of CD206-positive M2 cells in senescent BMDMs was significantly reduced compared to the young group. However, USP7 depletion rescued this reduction, but RAP partially antagonized the promoting M2 polarization effect of USP7 depletion (Fig. 4F). Further, qPCR results revealed that USP7 depletion in BMDMs co-cultured with apoptotic cells significantly upregulated anti-inflammatory gene expression and downregulated pro-inflammatory gene expression. However, using RAP to inhibit LRP1 partially counteracted this effect (Fig.S4). Finally, we directly co-cultured BMDMs with aged BMSCs and performed ALP and ARS staining. The results showed that sole USP7 depletion in BMDMs or BMSCs promoted osteogenesis compared to the NC groups of BMDMs or BMSCs, but the group with simultaneous USP7 depletion in both BMDMs and BMSCs exhibited the strongest osteogenic ability. However, si*Lrp1*-mediated LRP1 depletion in BMDMs

weakened the osteogenic capacity compared to that in BMDMs without Lrp1 depletion (Fig.4G).

USP7 inhibition orchestrates EPSIN1/LRP1 pathway to enhance efferocytosis

Next, we delved deeper into the specific pathway through which USP7 promotes efferocytosis in senescent BMDMs. Previous research has shown that EPSIN1 in macrophages could mediate the ubiquitination and degradation of LRP1, thereby inhibiting efferocytosis (*18*). Additionally, within the USP family, USP9x is known to deubiquitinate EPSIN1 (*19*). These findings prompted us to investigate whether USP7 could regulate macrophage efferocytosis by modulating the EPSIN1/LRP1 pathway.

Firstly, besides constructing a USP7-depleted macrophage model, we also established macrophage models overexpressing HA-USP7 and Flag-EPSIN1. By using cycloheximide (CHX) to treat macrophages, we observed that under conditions of protein synthesis inhibition, EPSIN1 was gradually degraded. However, after overexpressing HA-USP7, the expression of EPSIN1 protein significantly increased (Fig. 5A). Conversely, USP7 depletion led to a marked decrease in EPSIN1 expression (Fig. 5B). Subsequently, through co-IP, we further confirmed the protein interaction between USP7 and EPSIN1, as well as between HA-USP7 and Flag-EPSIN1 (Fig. 5C-D)).

Furthermore, we found that in senescent BMDMs, both USP7 and EPSIN1 expression increased, while LRP1 expression decreased. USP7 depletion reversed this trend (Fig. 5E). Additionally, the ubiquitination level of EPSIN1 in senescent BMDMs decreased, but USP7 depletion significantly increased EPSIN1 ubiquitination levels (Fig. 5F). These findings suggest that EPSIN1 might be a substrate protein for USP7 deubiquitination.

Next, we explored the interaction and ubiquitination status of the HA-USP7 and Flag-EPSIN1 system. The results revealed that the overexpression of these proteins did not affect the overall ubiquitin protein levels within the cells (Fig. 5G). However, in BMDMs overexpressing HA-USP7, the ubiquitination level of FLAG-EPSIN1 significantly decreased, indicating that HA-USP7 also possesses the ability to deubiquitinate Flag-EPSIN1 (Fig. 5H).

In summary, the results above suggested that there might be an abnormally high expression of USP7 in senescent BMDMs, leading to deubiquitination and reduced degradation of EPSIN1, subsequently resulting in excessive degradation of LRP1 and inhibition of efferocytosis. Knocking down USP7 increases EPSIN1 ubiquitination levels and degradation, thus allowing LRP1 to be protected from degradation and facilitating efferocytosis (Fig. 5I).

USP7 inhibition promotes osteoporosis in aged mice

To validate the *in vivo* effects of USP7 inhibition, we investigated the impact of USP7 inhibition on age-related osteoporosis. Firstly, after P5091 injection, MicroCT revealed a significant increase in bone mass in the femurs of aged mice, while changes in trabecular bone structure were not significant. However, co-administration of P5091

with the LRP1 inhibitor RAP reversed the promoting effect of P5091 (Fig. 6A-B). In the thoracic vertebrae, we observed that P5091 significantly increased bone mass and trabecular number, but RAP attenuated the therapeutic effect of P5091 (Fig. S5A-B).

Furthermore, HE staining of mouse femurs showed a significant increase in trabecular number on both sides of the metaphysis after P5091 injection in aged mice (Fig. S5C). Bone double-labeling fluorescence staining also indicated a noticeable increase in mineralization deposition area and rate in aged mice after P5091 injection (Fig. 6C). Combined with the results of ALP immunohistochemical staining, we found that this might be related to an increase in osteoblast numbers in trabecular bone following P5091 injection (Fig. 6D). We further examined femur samples through qPCR, which showed elevated expression of *Alp*, *Runx2*, and *Col1a1* in aged femurs tissue after P5091 injection, while RAP intervened in these treatment effects (Fig. 6E).

We also assessed the systemic effects of P5091 injection in mice. We found that P5091 significantly reduced the levels of IL-1β and IL-6 in the serum of aged mice and simultaneously decreased the area of lipid droplets in the liver of aged mice (Fig. 6F, Fig. S5C). These findings indicate that P5091 has therapeutic effects on other markers of aging in the systemic level of aged mice. However, unlike in bone tissue, RAP did not affect the efficacy of P5091 in other parts of the body.

USP7 inhibition promotes senolysis and efferocytosis in femurs of aged mice

Furthermore, we investigated whether P5091 could promote efferocytosis in bone tissue. We used TUNEL staining to label apoptotic cells and used F4/80 and DAPI to label macrophages to observe the phenomenon of macrophages engulfing apoptotic cells (Fig. 7A). We found that in the femoral tissue of aged mice, the numbers of apoptotic cells and macrophages were significantly reduced. P5091 significantly increased the numbers of apoptotic cells and macrophages in aged mice, but RAP did not affect the induction of apoptosis and the increase in macrophage numbers by P5091 (Fig. 7B-C). At the same time, the efferocytosis function in femoral tissue of aged mice was significantly weakened, but P5091 significantly increased the ratio of macrophages engulfing apoptotic cells. However, the application of RAP significantly attenuated the efferocytosis-promoting effect of P5091 (Fig. 7D).

DISCUSSION

In this study, we found that USP7 inhibition could suppress inflammaging in senescent BMDMs and mediate a senolytic effect on aged BMSCs. Moreover, these two effects, enhanced by USP7 depletion, were functionally interconnected by promoting macrophage efferocytosis via EPSIN1/LRP1 pathway, collectively facilitating osteogenic differentiation in aged BMSCs and suppressing SASP. Simultaneously, *in vivo* USP7 inhibition in mice promoted the alleviation of osteoporosis, which was associated with augmented senolysis and efferocytosis.

USP7 is a highly conserved protein in eukaryotic cells, and recent research has primarily focused on its role in influencing tumorigenesis and neurodegenerative diseases by modulating the MDM2/p53 pathway (*20*, *21*). In these diseases, USP7, as a convergence point for tumorigenesis, cellular senescence, and inflammatory responses,

has been extensively studied. USP7 is highly expressed in prostate, cervical, and colorectal cancers and is positively correlated with the worse survival of patients (*22-24*). Furthermore, USP7 has also been found to stabilize Tip60 and Foxp3, thereby promoting Treg function, suppressing immune responses, and facilitating tumor development (*25, 26*). As for neurodegenerative diseases, the loss of USP7 has been found to alleviate neuroinflammation in Parkinson's disease by downregulating Keap1 and upregulating NRF1 (*21*). Hence, various USP7 small molecule inhibitors are being studied and developed for cancer therapy and anti-inflammatory drugs. P5091, used in this study, is a selective inhibitor that significantly inhibits USP7 activity at a concentration of 4.2 μM (*27*). P5091 has been demonstrated to induce apoptosis of tumor cells in various types of cancer, such as colorectal cancer, ovarian cancer, and Ewing sarcoma, by regulating the p53/p21 pathway (*28, 29*). While studies have shown that USP7 inhibition could improve OVX-induced osteoporosis by suppressing osteoclast differentiation, the mechanisms underlying bone modeling in the context of aging remain to be investigated (*30*).

In this study, we initially investigated the effects of USP7 inhibition on the inflammaging of BMDMs. In this study, we initially observed that the conditioned media from aged BMSCs could upregulate the expression of inflammatory cytokines such as IL-1β, IL-6, and TNF-α in BMDMs. This conditioned media also enhanced NLRP3 inflammasome pathway, indicating inflammaging in BMDMs. Next, we found that USP7 could downregulate the innate immune response pathway and NLRP3 inflammasome pathway in senescent BMDMs. Similar to our findings, Palazon et al. discovered that USP7 and USP47 directly regulated the deubiquitination of NLRP3 protein and mainly maintained the NLRP3 pathway by preserving ASC speck formation (*31*). However, there is a slight difference between our results and those of Palazon et al. They found that inhibiting USP7 and USP47 had little impact on the protein levels of pro-CASP1, whereas we observed a significant downregulation of pro-CASP1 protein levels after USP7 inhibition. This difference may be attributed to variations in the experimental approaches. We utilized USP7 depletion and USP7 inhibitor P5091, while Palazon et al. employed a combined inhibition of USP7 and USP47. Additionally, in contrast to Palazon et al.'s use of LPS and nigericin to stimulate cells, we used conditioned media from aged BMSCs to induce M1 polarization in macrophages. This difference in stimulation may activate signaling pathways other than NLRP3, such as the NLRC4 inflammasome pathway which also can activate pro-CASP1 (*32*). Furthermore, in chondrocytes, USP7 inhibition has been shown to promote the ubiquitination of NOX4, thereby reducing oxidative stress and mitigating joint damage in osteoarthritis (*33*). Therefore, future researches may focus on exploring the role of USP7 in inhibiting inflammation in the inflammatory microenvironment of age-related osteoporosis, particularly in different cell types. Additionally, specific cellular pathways, such as the inflammasome pathways involving NLRC4 and AIM2 in addition to NLRP3, may also warrant investigations.

After validating the regulatory effect of USP7 on BMDMs' inflammaging, we further investigated the impact of USP7 on BMSCs-BMDMs crosstalk. After USP7 depletion, BMDMs relieved their inhibitory effect on aged BMSCs' osteogenesis. Additionally,

based on SA-β-gal staining, we found that USP7 depletion in BMDMs reduced the number of aged BMSCs. Furthermore, PCR results indicated that USP7 depletion in BMDMs downregulated SASP markers in aged BMSCs. In previous studies, it was found that IL-6 and TNF-α secreted by M1 macrophages significantly inhibited the functions of BMSCs and osteoblasts (*34, 35*). Li and colleagues discovered that in the bone marrow of aged mice, 80% of macrophages exhibit the M1 phenotype (whereas in young mice, M1 macrophages only make up 5%), and GCA secreted by these M1 macrophages significantly inhibited osteogenic differentiation (*36*). It primarily causes bone loss through three pathways. First, it can promote the differentiation of monocyte lineage into osteoclasts, leading to bone resorption (*37*). Second, it can directly inhibit BMSCs osteogenic differentiation and osteoblast function, reducing bone formation (*38*). Third, it can further enhance the inflammatory response by promoting other immune cells such as neutrophils and T cells, *etc* (*39*). Therefore, inhibiting the inflammatory response of macrophages is an important approach in treating age-related osteoporosis. However, some studies have found that M1 macrophages could promote early bone healing by secreting factors like OSM (Oncostatin M) and PGE2 (Prostaglandin E2) (*40-42*). Therefore, further research is needed to explore the role of M1 macrophages in age-related bone healing.

Besides, in age-related osteoporosis, the excessive inflammatory response of macrophages is also influenced by external factors. In osteocytes, p53/p16 can mediate cellular senescence, leading to the production of SASP markers such as IL-1α and IL-6, which contribute to the formation of inflammatory microenvironment (*43*). p53, as a crucial regulator of aging and apoptosis, also plays a significant role in the inflammatory pathways (*44*). Therefore, in order to selectively induce apoptosis in senescent cells and reduce SASP-induced damage to neighboring cells, senolytic drugs that through p53 modulation holds significant research potential. He et al. utilized ionizing radiation-induced senescent fibroblasts and found that the USP7 inhibitor P5091 functions as a senolytic drug by inducing apoptosis in senescent cells through the modulation of the MDM2/p53 pathway (*15*). Inspired by these findings, we discovered that USP7 depletion promoted apoptosis and osteoblast differentiation in aged BMSCs, while SASP pathway was inhibited. Further, we found that USP7 inhibition could selectively induce apoptosis in aged BMSCs. Therefore, we validated P5091, as a potential senolytic drug, that might also affect aged BMSCs and promoted osteogenic capabilities. Furthermore, it is noteworthy that we observed that USP7 depletion, while increasing the mRNA expression of *Alp*, *Runx2*, and *Col1a1* in young BMSCs, led to a reduction in the protein levels of ALP and COL1A1. This suggested that USP7 might be involved in post-transcriptional regulation mechanisms for ALP and COL1A1 proteins. Additionally, ALP/ARS staining revealed that USP7 inhibition had the most pronounced inhibitory effect on the mineralization phase of young BMSCs. Similarly, Kim et al. demonstrated that after USP7 depletion, the ubiquitination levels of NANOG and SOX2 increased, subsequently inhibiting self-renewal capacity and multipotency of BMSCs (*45*). Therefore, the role USP7 inhibition in osteogenesis of young and aged BMSCs require further exploration.

While inducing apoptosis in senescent cells is a promising therapeutic approach, excessive cell apoptosis can also impact bone remodeling (*46*). Under physiological conditions, apoptotic cells are selectively engulfed by macrophages in a process known as efferocytosis (*47*). Efferocytosis consists of three stages: the smell phase, the eating phase, and the digestion phase. After completing efferocytosis, macrophages undergo M2 polarization and produce anti-inflammatory cytokines (*48*). Indeed, this is crucial for wound healing and tissue homeostasis. Efferocytosis plays a critical role in transitioning M1 macrophages into the M2 phenotype, which contributes to tissue remodeling in the later stages of wound healing (*49-50*). However, in aging individuals, macrophages may experience impaired phagocytic and efferocytosis functions because of impaired MerTK function (*51*). In this study, we observed that USP7 depletion improved the impaired efferocytosis function of senescent BMDMs and significantly promoted the polarization of macrophages towards the M2 phenotype. Furthermore, in direct co-culture experiments with aged BMSCs and BMDMs, we found that the osteogenic effect was more pronounced when USP7 was simultaneously depleted in both BMSCs and BMDMs, as compared to when it was only depleted in aged BMSCs or BMDMs. This suggested a synergistic effect of the increased senolysis level in aged BMSCs and the enhanced efferocytosis level in senescent BMDMs.

At the same time, we noticed a decrease in the expression levels of *Lrp1* in aging BMDMs. LRP1 is a key receptor involved in mediating efferocytosis (*52*). In atherosclerosis, LRP1 in monocytes is degraded through EPSIN1-mediated mechanisms, leading to a reduction in efferocytosis (*18*). Therefore, we used an LRP1 inhibitor RAP and found that LRP1 inhibition could counteract the promoting effect of USP7 on efferocytosis. Subsequently, we investigated how USP7 regulates LRP1 and found that USP7 inhibition could increase the ubiquitination of EPSIN1, thus protecting LRP1 from degradation, and consequently enhancing the efferocytosis capacity of senescent BMDMs.

In *in vivo* experiments, we validated the impact of USP7 inhibitor P5091 on age-related osteoporosis of mice. We observed an increased number of apoptotic cells near the growth plate of femurs and an increase in bone mass in the femurs and vertebrae of aged mice following systemic administration of P5091. This suggests that systemic P5091 can alleviate osteoporosis in aged mice through senolysis. Similar to our findings, Farr et al. discovered that in the skeletal system of aged mice, the primary sources of SASP are osteocytes and myeloid lineage (*53*). Clearing senescent cells led to a significant increase in bone mass in the femurs and vertebrae of aged mice (*54*). However, Farr et al. further found that clearing senescent osteocytes alone could improve bone mass in vertebrae but not in the femurs. This suggests that the therapeutic effect of clearing senescent cells on osteoporosis may partially stem from reducing the overall burden of senescent cells throughout the body (*55*). Similarly, we observed that after systemic administration of P5091, the levels of pro-inflammatory cytokines IL-1β and IL-6 in the serum of aged mice decreased, and there was a reduction in lipid droplet area in the liver. This suggested that systemic injection of P5091 might partially function on the femurs and vertebrae by reducing the number of senescent cells in other parts of the body and exerting remote effects. Furthermore, we also observed that P5091 enhanced

efferocytosis efficiency in femurs. However, when we used RAP, as mentioned earlier, we found a significant reduction in efferocytosis levels. Additionally, bone mass in both the femur and vertebrae decreased, indicating that the efferocytosis inhibitor LRP1 might abolish the bone-improving effect of P5091. However, systemic markers, like IL-1β and IL-6 in the serum of aged mice were not altered by RAP. This could be attributed to the fact that LRP1 has an impact on osteoblasts as well. LRP1 on the surface of osteoblasts can limit osteoclast activation, thus reducing bone loss (*56*). Therefore, systemic injection of RAP may not only inhibit LRP1 on macrophages but also affect LRP1 on osteoblasts, leading to a more pronounced effect in the femur and vertebrae.

In summary, this study found that USP7 inhibition could enhance the impaired efferocytosis capacity of senescent BMDMs and promote senolytic effect in aged BMSCs. Efferocytosis and senolysis play a synergistic role in the interaction between BMSCs and BMDMs, where USP7-induced apoptosis in senescent cells can be efficiently cleared by macrophages through efferocytosis. This "kill and bury" mechanism holds promise for future drug design and combination therapy strategies. However, this study still has several limitations. For example, in *in vivo* experiments, there may be other immune cells, such as dendritic cells, participating in efferocytosis, but this study only explored macrophages. Besides, *in vivo* experiments should further investigate the effects of the drug on other aging tissues and their remote effects. As for *in vitro*, further researches should delve into the molecular mechanisms underlying USP7's regulation of senolysis in aged BMSCs. Additionally, due to the limitations of the direct co-culture model for WB and qPCR detection, some experiments used an indirect co-culture model with transwells, which has certain limitations in studying efferocytosis as macrophages can only interact with BMSCs through paracrine processes.

REFERENCES

1. Lane NE. Epidemiology, etiology, and diagnosis of osteoporosis. Am J Obstet Gynecol. 2006;194(2 Suppl):S3-11.
2. Saxena Y, Routh S, Mukhopadhaya A. Immunoporosis: Role of Innate Immune Cells in Osteoporosis. Front Immunol. 2021;12:687037.
3. Anam AK, Insogna K. Update on Osteoporosis Screening and Management. Med Clin North Am. 2021;105(6):1117-34.
4. Reid IR, Billington EO. Drug therapy for osteoporosis in older adults. Lancet. 2022;399(10329):1080-92.
5. He LH, Xiao E, An JG, He Y, Chen S, Zhao L, et al. Role of Bone Marrow Stromal Cells in Impaired Bone Repair from BRONJ Osseous Lesions. J Dent Res. 2017;96(5):539-46.
6. Bellavia D, Costa V, De Luca A, Maglio M, Pagani S, Fini M, et al. Vitamin D Level Between Calcium-Phosphorus Homeostasis and Immune System: New Perspective in Osteoporosis. Curr Osteoporos Rep. 2016.
7. Ferbebouh M, Vallières F, Benderdour M, Fernandes J. The pathophysiology of immunoporosis: innovative therapeutic targets. Inflamm Res. 2021;70(8):859-75.

8. Srivastava RK, Dar HY, Mishra PK. Immunoporosis: Immunology of Osteoporosis-Role of T Cells. Front Immunol. 2018;9:657.
9. Zhang W, Gao R, Rong X, Zhu S, Cui Y, Liu H, et al. Immunoporosis: Role of immune system in the pathophysiology of different types of osteoporosis. Front Endocrinol (Lausanne). 2022;13:965258.
10. Ferrucci L, Fabbri E. Inflammageing: chronic inflammation in ageing, cardiovascular disease, and frailty. Nat Rev Cardiol. 2018;15(9):505-22.
11. Park J, Cho J, Song EJ. Ubiquitin-proteasome system (UPS) as a target for anticancer treatment. Arch Pharm Res. 2020;43(11):1144-61.
12. Li Q, Zhou L, Qin S, Huang Z, Li B, Liu R, et al. Proteolysis-targeting chimeras in biotherapeutics: Current trends and future applications. Eur J Med Chem. 2023;257:115447.
13. Komander D, Clague MJ, Urbé S. Breaking the chains: structure and function of the deubiquitinases. Nat Rev Mol Cell Biol. 2009;10(8):550-63.
14. Lange SM, Armstrong LA, Kulathu Y. Deubiquitinases: From mechanisms to their inhibition by small molecules. Mol Cell. 2022;82(1):15-29.
15. He Y, Li W, Lv D, Zhang X, Zhang X, Ortiz YT, et al. Inhibition of USP7 activity selectively eliminates senescent cells in part via restoration of p53 activity. Aging cell. 2020;19(3):e13117.
16. Schmitt R. Senotherapy: growing old and staying young? Pflugers Archiv : European journal of physiology. 2017;469(9):1051-9.
17. Schilperoort M, Ngai D, Katerelos M, Power DA, Tabas I. PFKFB2-mediated glycolysis promotes lactate-driven continual efferocytosis by macrophages. Nat Metab. 2023;5(3):431-44.
18. Brophy ML, Dong Y, Tao H, Yancey PG, Song K, Zhang K, et al. Myeloid-Specific Deletion of Epsins 1 and 2 Reduces Atherosclerosis by Preventing LRP-1 Downregulation. Circ Res. 2019;124(4).
19. Chen H, Polo S, Di Fiore PP, De Camilli PV. Rapid Ca2+-dependent decrease of protein ubiquitination at synapses. Proceedings of the National Academy of Sciences of the United States of America. 2003;100(25):14908-13.
20. Qi S-M, Cheng G, Cheng X-D, Xu Z, Xu B, Zhang W-D, et al. Targeting USP7-Mediated Deubiquitination of MDM2/MDMX-p53 Pathway for Cancer Therapy: Are We There Yet? Frontiers in cell and developmental biology. 2020;8:233.
21. Zhang X-W, Feng N, Liu Y-C, Guo Q, Wang J-K, Bai Y-Z, et al. Neuroinflammation inhibition by small-molecule targeting USP7 noncatalytic domain for neurodegenerative disease therapy. Sci Adv. 2022;8(32):eabo0789.
22. An T, Gong Y, Li X, Kong L, Ma P, Gong L, et al. USP7 inhibitor P5091 inhibits Wnt signaling and colorectal tumor growth. Biochemical pharmacology. 2017;131:29-39.
23. Su D, Ma S, Shan L, Wang Y, Wang Y, Cao C, et al. Ubiquitin-specific protease 7 sustains DNA damage response and promotes cervical carcinogenesis. The Journal of clinical investigation. 2018;128(10):4280-96.

24. Xia X, Liao Y, Huang C, Liu Y, He J, Shao Z, et al. Deubiquitination and stabilization of estrogen receptor α by ubiquitin-specific protease 7 promotes breast tumorigenesis. Cancer letters. 2019;465:118-28.
25. Wang L, Kumar S, Dahiya S, Wang F, Wu J, Newick K, et al. Ubiquitin-specific Protease-7 Inhibition Impairs Tip60-dependent Foxp3+ T-regulatory Cell Function and Promotes Antitumor Immunity. EBioMedicine. 2016;13.
26. van Loosdregt J, Fleskens V, Fu J, Brenkman AB, Bekker CPJ, Pals CEGM, et al. Stabilization of the transcription factor Foxp3 by the deubiquitinase USP7 increases Treg-cell-suppressive capacity. Immunity. 2013;39(2):259-71.
27. Chauhan D, Tian Z, Nicholson B, Kumar KGS, Zhou B, Carrasco R, et al. A small molecule inhibitor of ubiquitin-specific protease-7 induces apoptosis in multiple myeloma cells and overcomes bortezomib resistance. Cancer Cell. 2012;22(3):345-58.
28. Fu C, Zhu X, Xu P, Li Y. Pharmacological inhibition of USP7 promotes antitumor immunity and contributes to colon cancer therapy. Onco Targets Ther. 2019;12:609-17.
29. Stolte B, Iniguez AB, Dharia NV, Robichaud AL, Conway AS, Morgan AM, et al. Genome-scale CRISPR-Cas9 screen identifies druggable dependencies in TP53 wild-type Ewing sarcoma. J Exp Med. 2018;215(8):2137-55.
30. Lin YC, Zheng G, Liu HT, Wang P, Yuan WQ, Zhang YH, Peng XS, Li GJ, Wu YF, Shen HY. USP7 promotes the osteoclast differentiation of CD14+ human peripheral blood monocytes in osteoporosis via HMGB1 deubiquitination. J Orthop Translat. 2023 Jun 11;40:80-91.
31. Palazón-Riquelme P, Worboys JD, Green J, Valera A, Martín-Sánchez F, Pellegrini C, et al. USP7 and USP47 deubiquitinases regulate NLRP3 inflammasome activation. EMBO reports. 2018;19(10).
32. Zhou F, Zhang G, Wu Y, Xiong Y. Inflammasome Complexes: Crucial mediators in osteoimmunology and bone diseases. Int Immunopharmacol. 2022;110:109072.
33. Liu G, Liu Q, Yan B, Zhu Z, Xu Y. USP7 Inhibition Alleviates H2O2-Induced Injury in Chondrocytes via Inhibiting NOX4/NLRP3 Pathway. Frontiers in pharmacology. 2020;11:617270.
34. Harmer D, Falank C, Reagan MR. Interleukin-6 Interweaves the Bone Marrow Microenvironment, Bone Loss, and Multiple Myeloma. Front Endocrinol (Lausanne). 2018;9:788.
35. Sun W, Meednu N, Rosenberg A, Rangel-Moreno J, Wang V, Glanzman J, et al. B cells inhibit bone formation in rheumatoid arthritis by suppressing osteoblast differentiation. Nature communications. 2018;9(1):5127.
36. Li C-J, Xiao Y, Sun Y-C, He W-Z, Liu L, Huang M, et al. Senescent immune cells release grancalcin to promote skeletal aging. Cell metabolism. 2021;33(10).
37. Champagne CM, Takebe J, Offenbacher S, Cooper LF. Macrophage cell lines produce osteoinductive signals that include bone morphogenetic protein-2. Bone. 2002;30(1):26-31.
38. Zhou M, Graves DT. Impact of the host response and osteoblast lineage cells on periodontal disease. Front Immunol. 2022;13:998244.

39. Okamoto K, Nakashima T, Shinohara M, Negishi-Koga T, Komatsu N, Terashima A, et al. Osteoimmunology: The Conceptual Framework Unifying the Immune and Skeletal Systems. Physiol Rev. 2017;97(4):1295-349.
40. Guihard P, Danger Y, Brounais B, David E, Brion R, Delecrin J, et al. Induction of osteogenesis in mesenchymal stem cells by activated monocytes/macrophages depends on oncostatin M signaling. Stem Cells. 2012;30(4):762-72.
41. Philipp D, Suhr L, Wahlers T, Choi Y-H, Paunel-Görgülü A. Preconditioning of bone marrow-derived mesenchymal stem cells highly strengthens their potential to promote IL-6-dependent M2b polarization. Stem cell research & therapy. 2018;9(1):286.
42. Liu Z, Yuan X, Liu M, Fernandes G, Zhang Y, Yang S, et al. Antimicrobial Peptide Combined with BMP2-Modified Mesenchymal Stem Cells Promotes Calvarial Repair in an Osteolytic Model. Molecular therapy : the journal of the American Society of Gene Therapy. 2018;26(1):199-207.
43. Xu L, Wang Y, Wang J, Zhai J, Ren L, Zhu G. Radiation-Induced Osteocyte Senescence Alters Bone Marrow Mesenchymal Stem Cell Differentiation Potential via Paracrine Signaling. International journal of molecular sciences. 2021;22(17).
44. Nacarelli T, Lau L, Fukumoto T, Zundell J, Fatkhutdinov N, Wu S, et al. NAD+ metabolism governs the proinflammatory senescence-associated secretome. Nature cell biology. 2019;21(3):397-407.
45. Kim YJ, Park KH, Lee K-M, Chun Y-M, Lee JW. Deubiquitinating Enzyme USP7 Is Required for Self-Renewal and Multipotency of Human Bone Marrow-Derived Mesenchymal Stromal Cells. International journal of molecular sciences. 2022;23(15).
46. Bran GM, Stern-Straeter J, Hörmann K, Riedel F, Goessler UR. Apoptosis in bone for tissue engineering. Arch Med Res. 2008;39(5):467-82.
47. Mehrotra P, Ravichandran KS. Drugging the efferocytosis process: concepts and opportunities. Nat Rev Drug Discov. 2022;21(8):601-20.
48. Boada-Romero E, Martinez J, Heckmann BL, Green DR. The clearance of dead cells by efferocytosis. Nat Rev Mol Cell Biol. 2020;21(7):398-414.
49. Kim H, Wang SY, Kwak G, Yang Y, Kwon IC, Kim SH. Exosome-Guided Phenotypic Switch of M1 to M2 Macrophages for Cutaneous Wound Healing. Adv Sci (Weinh). 2019;6(20):1900513.
50. Maschalidi S, Mehrotra P, Keçeli BN, De Cleene HKL, Lecomte K, Van der Cruyssen R, et al. Targeting SLC7A11 improves efferocytosis by dendritic cells and wound healing in diabetes. Nature. 2022;606(7915):776-84.
51. Rymut N, Heinz J, Sadhu S, Hosseini Z, Riley CO, Marinello M, et al. Resolvin D1 promotes efferocytosis in aging by limiting senescent cell-induced MerTK cleavage. FASEB journal : official publication of the Federation of American Societies for Experimental Biology. 2020;34(1):597-609.
52. Doddapattar P, Dev R, Ghatge M, Patel RB, Jain M, Dhanesha N, et al. Myeloid Cell PKM2 Deletion Enhances Efferocytosis and Reduces Atherosclerosis. Circ Res. 2022;130(9):1289-305.

53. Farr JN, Fraser DG, Wang H, Jaehn K, Ogrodnik MB, Weivoda MM, et al. Identification of Senescent Cells in the Bone Microenvironment. J Bone Miner Res. 2016;31(11):1920-9.
54. Farr JN, Xu M, Weivoda MM, Monroe DG, Fraser DG, Onken JL, et al. Targeting cellular senescence prevents age-related bone loss in mice. Nat Med. 2017;23(9):1072-9.
55. Farr JN, Saul D, Doolittle ML, Kaur J, Rowsey JL, Vos SJ, et al. Local senolysis in aged mice only partially replicates the benefits of systemic senolysis. The Journal of clinical investigation. 2023;133(8).
56. Bartelt A, Behler-Janbeck F, Beil FT, Koehne T, Müller B, Schmidt T, et al. Lrp1 in osteoblasts controls osteoclast activity and protects against osteoporosis by limiting PDGF-RANKL signaling. Bone Res. 2018;6:4.

Materials and methods：Materials and methods were described in the supplementary information.

Acknowledgments: We acknowledge the funding from the National Natural Science Foundation of China (81970966, 82001084), Natural Science Foundation of Sichuan Province (2023NSFSC1513, 2023NSFSC0574).

Author contributions:

Conceptualization: FZ
Methodology: FZ, FB, GZ
Investigation: FZ, ZW, HY
Visualization: FZ, QW, WL
Funding acquisition: YX, YW
Project administration: FZ, ZW, DW
Supervision: YX, YW
Writing – original draft: FZ, ZW
Writing – review & editing: FZ

Declaration of interests: Authors declare that they have no competing interests.

Declaration of Generative AI and AI-assisted technologies in the writing process: During the preparation of this work the authors used chatGPT 3.5 in order to edit English writing. After using this tool, the authors reviewed and edited the content as needed and take full responsibility for the content of the publication.

Data and materials availability: The data that support the findings of this study are available on request from the corresponding author upon reasonable request.

Figures

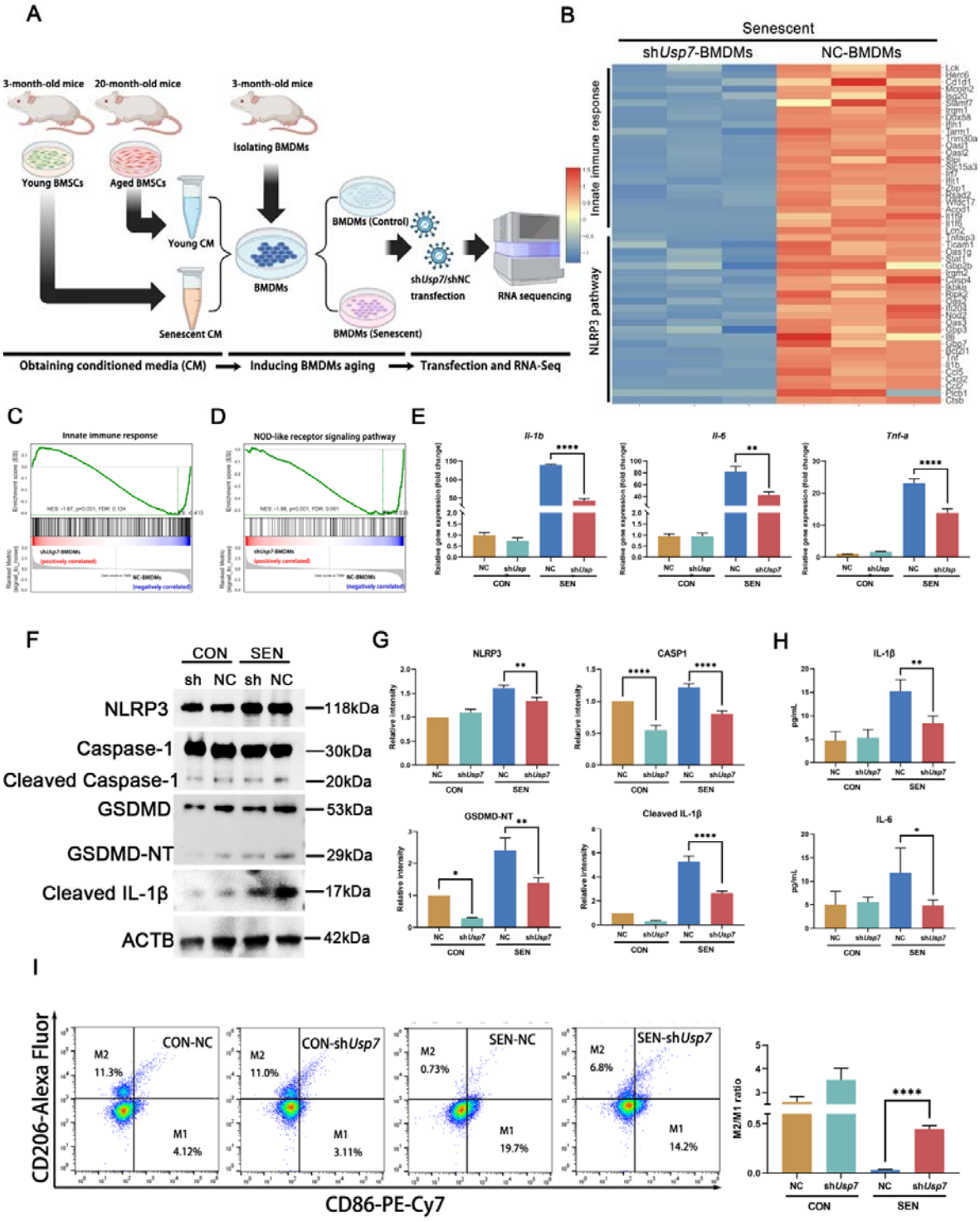
A
3-month-old mice
20-month-old mice
3-month-old mice
Isolating BMDMs
Young BMSCs
Aged BMSCs
Young CM
Senescent CM
BMDMs
BMDMs (Control)
BMDMs (Senescent)
shUsp7/shNC transfection
RNA sequencing
Obtaining conditioned media (CM)
Inducing BMDMs aging
Transfection and RNA-Seq
B
Senescent
shUsp7-BMDMs
NC-BMDMs
Innate immune response
NLRP3 pathway
C
Innate immune response
D
NOD-like receptor signaling pathway
E
Il-1b
Il-6
Tnf-a
CON
SEN
F
CON
SEN
sh
NC
NLRP3
Caspase-1
Cleaved Caspase-1
GSDMD
GSDMD-NT
Cleaved IL-1β
ACTB
118kDa
30kDa
20kDa
53kDa
29kDa
17kDa
42kDa
G
NLRP3
CASP1
GSDMD-NT
Cleaved IL-1β
H
IL-1β
IL-6
I
CD206-Alexa Fluor
CD86-PE-Cy7
CON-NC
CON-shUsp7
SEN-NC
SEN-shUsp7
M2
11.3%
M1
4.12%
M2
11.0%
M1
3.11%
M2
0.73%
M1
19.7%
M2
6.8%
M1
14.2%
M2/M1 ratio

Fig. 1. **USP7 depletion inhibited inflammaging in senescent BMDMs via NLRP3 inflammasome pathway.** (**A**) Illustration of the experimental workflow for acquiring senescent BMDMs, USP7 depletion, and RNA-Seq. (**B**) Heatmap of representative core genes associated with innate immune response and NLRP3 inflammasome pathway. (**C-D**) GSEA showed downregulated innate immune response and NLRP3 inflammasome pathway in USP7-depleted senescent BMDMs. (E) qPCR results of maker genes of inflammaging in normal/senescent BMDMs transfected with sh*Usp7* or NC for 4 d, *n*=3. (**F**) Western blot and (**G**) quantification of NLRP3, Caspase-1, GSDMD, IL-1β and β-actin in different group of BMDMs transfected with sh*Usp7* or NC for 4 d, *n*=3. (**H**) ELISA showed the production of IL-1β and IL-6 in supernatant of normal/senescent BMDMs transfected with sh*Usp7* or NC for 4 d, *n*=3. (**I**) Flow cytometry analysis for M2/M1 polarization of normal/senescent BMDMs transfected with sh*Usp7* or NC for 4 d, *n*=3. CON, control BMDMs; SEN, senescent BMDMs; NC, BMDMs transfected with NC lentivirus; sh*Usp7*, BMDMs transfected with sh*Usp7* lentivirus. Data are presented as means ± SD. **P* < 0.05, ***P* < 0.01, ****P* < 0.001, *****P* < 0.0001.

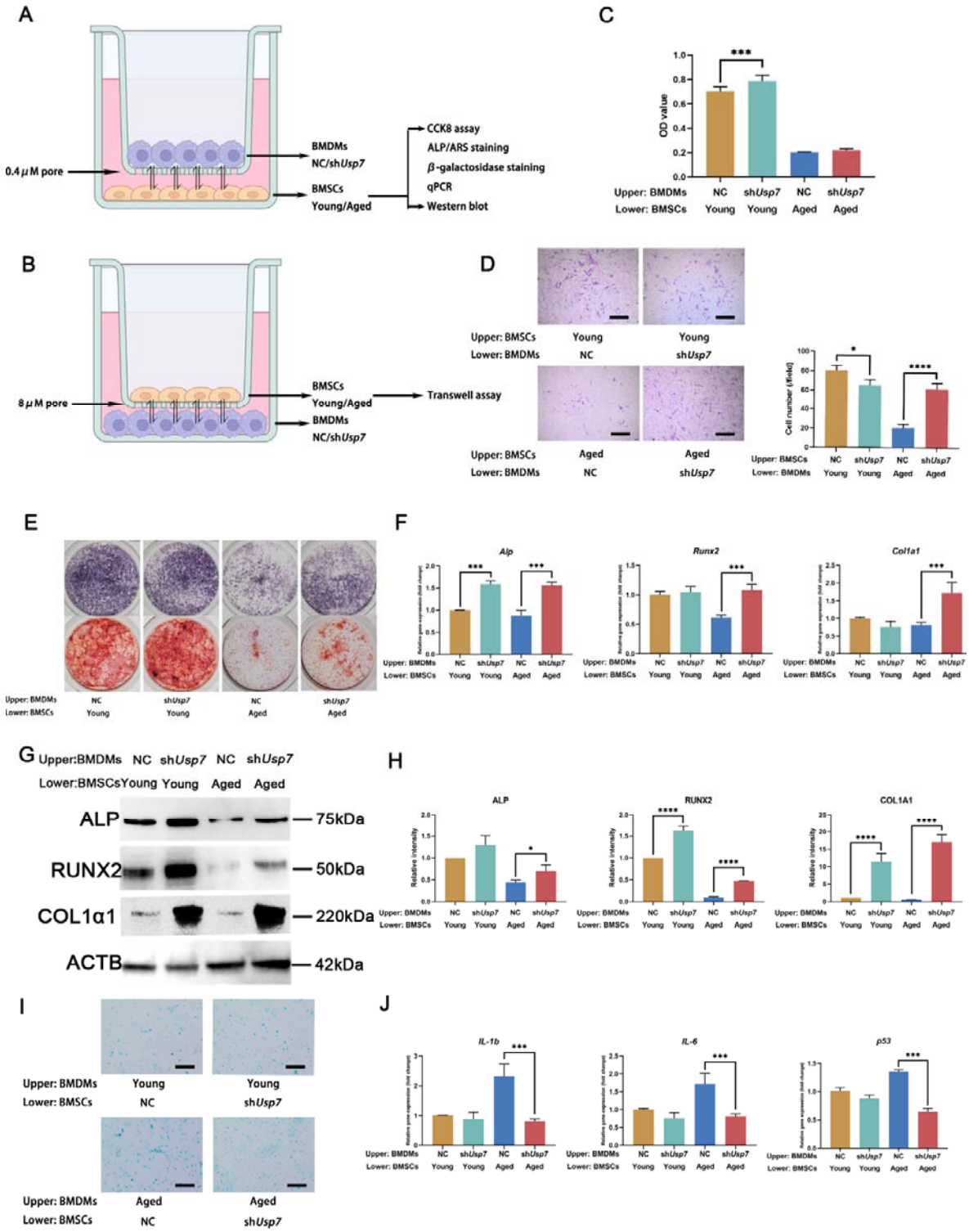

Fig. 2. **USP7-depleted BMDMs enhanced osteogenesis of aged BMSCs.** (**A-B**) Illustration of the indirect co-culture model of BMSCs and BMDMs for CCK8 assay, ALP/ARS staining, SA-β-gal staining, qPCR, Western blot, and transwell assay. (**C**) CCK8 assay for determining cell viability of young/aged BMSCs

co-cultured with different BMDMs for 72 h, *n*=6. (**D**) Representative images and quantitative analysis of migration capacity of aged/young BMSCs co-cultured with different BMDMs for 24 h, *n*=3, scale bar, 50μM. (**E**) Representative images of ALP and ARS staining in different groups of BMSCs after initiating osteogenic induction for 7 and 14 d. (**F**) qPCR results of osteogenic markers in different groups of BMSCs after initiating osteogenic induction for 7 d, *n*=3. (**G**) Western blot and (**H**) quantification of ALP, RUNX2, COL1α1, and β-actin in different group of BMSCs after initiating osteogenic induction for 7 d, *n*=3. (**I**) Representative images of β-galactosidase staining of different BMSCs, scale bar, 50μM. (**J**) qPCR results of SASP markers in different groups of BMSCs, *n*=3. NC, BMDMs transfected with NC lentivirus; sh*Usp7*, BMDMs transfected with sh*Usp7* lentivirus. Data are presented as means ± SD. **P* < 0.05, ***P* < 0.01, ****P* < 0.001, *****P* < 0.0001.

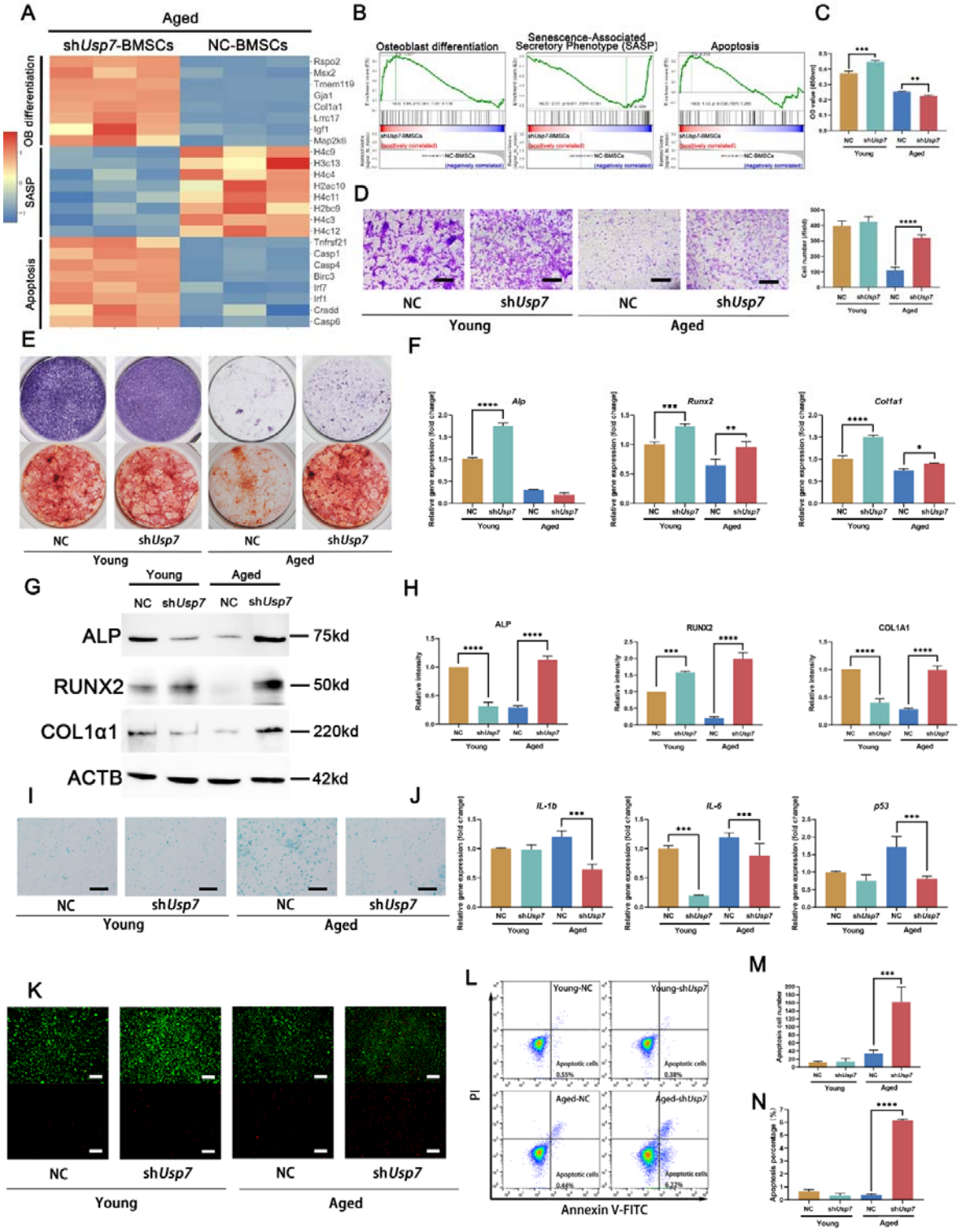

Fig. 3. **USP7 depletion promoted osteogenesis of aged BMSCs via senolysis.** (**A**) Heatmap of representative core genes associated with osteoblast differentiation, SASP, and apoptosis pathway. (**B**) GSEA showed upregulated osteoblast differentiation, downregulated SASP and apoptosis pathway in USP7-depleted

aged BMSCs. (**C**) CCK8 assay for determining cell viability of young/aged BMSCs transfected with NC or sh*Usp7* lentivirus for 72 h, *n*=6. (**D**) Representative images and quantitative analysis of migration capacity of aged/young BMSCs for 24 h, *n*=3, scale bar, 50μM. (**E**) Representative images of ALP and ARS staining in different groups of BMSCs after initiating osteogenic induction for 7 and 14 d. (**F**) qPCR results of osteogenic markers in different groups of BMSCs after initiating osteogenic induction for 7 d, *n*=3. (**G**) Western blot and (**H**) quantification of ALP, RUNX2, COL1α1, and β-actin in different group of BMSCs after initiating osteogenic induction for 7 d, *n*=3. (**I**) Representative images of SA-β-gal staining of different BMSCs, scale bar, 50μM. (**J**) qPCR results of SASP markers in different groups of BMSCs, *n*=3. (**K**) Representative images of live/dead staining of BMSCs after transfected with NC or sh*Usp7* lentivirus for 72 h, green color indicates live cells, red color indicates dead cells, scale bar, 150μM. (**L**) Flow cytometry for apoptosis in BMSCs after transfected with NC or sh*Usp7* lentivirus for 72 h. (**M-N**) Quantification of live/dead staining and flow cytometry to evaluate apoptosis and senolysis level in BMSCs, *n*=3. NC, BMSCs transfected with NC lentivirus; sh*Usp7*, BMSCs transfected with sh*Usp7* lentivirus. Data are presented as means ± SD. *$P < 0.05$, **$P < 0.01$, ***$P < 0.001$, ****$P < 0.0001$.

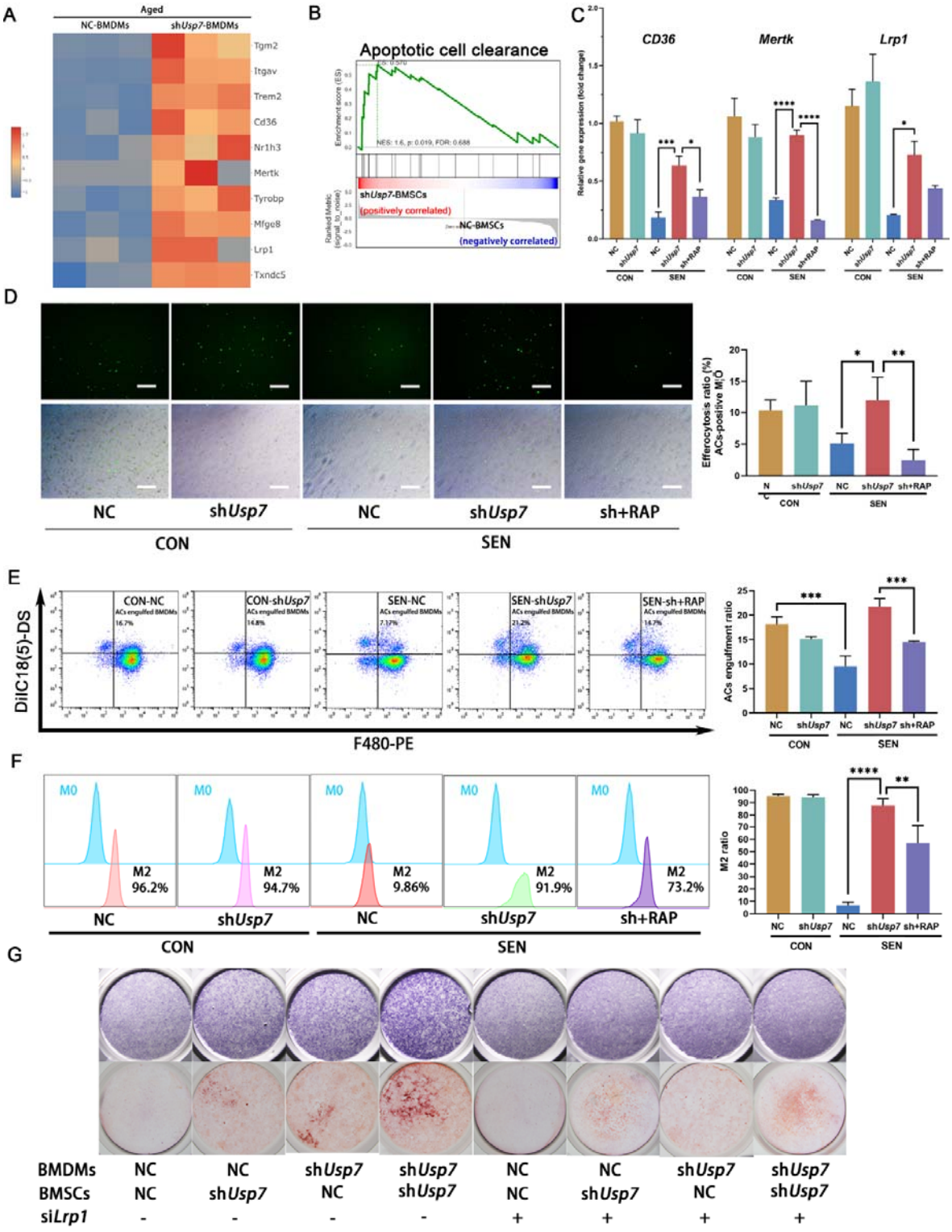

Fig. 4. **USP7 depletion promoted efferocytosis in senescent BMDMs partially through LRP1** (**A**) Heatmap of representative core genes associated with apoptotic cell clearance. (**B**) GSEA showed upregulated apoptotic clearance

pathway in USP7-depleted aged BMDMs. (**C**) qPCR results of efferocytosis markers in different groups of normal/senescent BMDMs transfected with sh*Usp7* or NC for 4 d, *n*=3. (**D**) Representative images and quantitative analysis of efferocytosis ratio control/senescent BMDMs co-cultured with apoptotic Jurkat cells for 24 h, *n*=3, scale bar, 150μM. (**E**) Flow cytometry analysis for evaluating efferocytosis capacity of control/senescent BMDMs co-cultured with apoptotic Jurkat cells for 24 h, *n*=3. (**F**) Flow cytometry analysis for evaluating M2 polarization ratio of control/senescent BMDMs co-cultured with apoptotic Jurkat cells for 24 h, *n*=3. (**G**) ALP and ARS staining of BMSCs directly co-cultured with BMDMs after initiating osteogenic induction for 7 and 14 d. CON, control BMDMs; SEN, senescent BMDMs; NC, BMDMs transfected with NC lentivirus; sh*Usp7*, BMDMs transfected with sh*Usp7* lentivirus. RAP, receptor associated protein. Data are presented as means ± SD. *$P < 0.05$, **$P < 0.01$, ***$P < 0.001$, ****$P < 0.0001$.

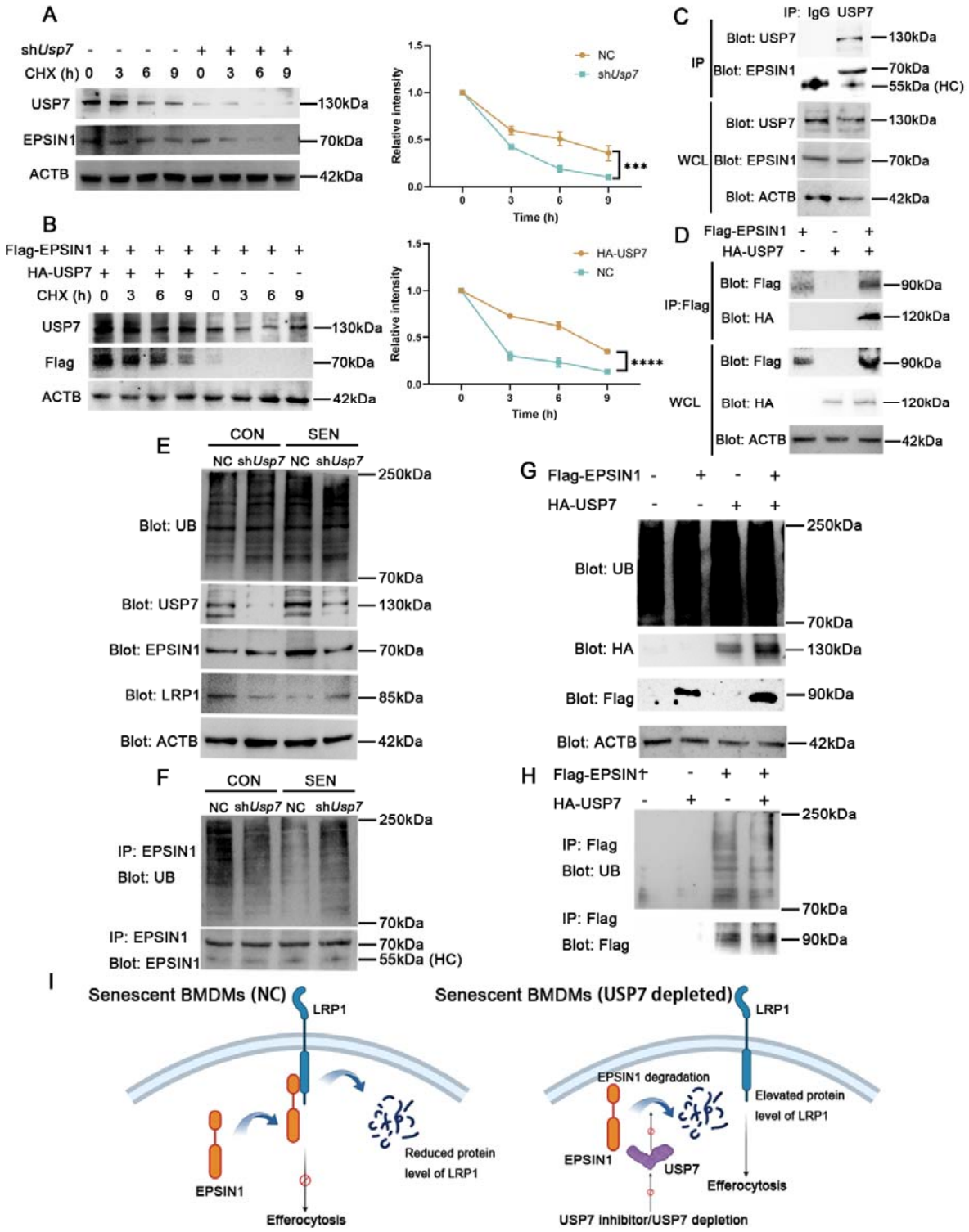

Fig. 5. **USP7 depletion mediated ubiquitin-dependent degradation of EPSIN1 to stabilize LRP1** Immunoblot of EPSIN1 in BMDMs when USP7 was overexpressed (**A**) or depleted (**B**) genetically with 20 μmol/L CHX for different times as indicated. (**C**) Interaction analysis of USP7 and EPSIN1 in BMDMs

was detected using co-IP. (**D**) BMDMs was transfected with HA-USP7 and Flag-EPSIN1. Interaction of HA-USP7 and Flag-EPSIN1 was detected using co-IP. (**E**) Immunoblot analysis of ubiquitin, USP7, EPSIN1, and LRP1 in control/senescent BMDMs transfected with NC of sh*Usp7* lentivirus, followed by (**F**) co-IP with anti-EPSIN1, probed with anti-ubiquitin and anti-EPSIN1 in control/senescent BMDMs transfected with NC of sh*Usp7* lentivirus. (**G**) Immunoblot analysis of ubiquitin, HA, and Flag in BMDMs transfected with FLAG-EPSIN1, HA-USP7 and both, followed by (**H**) co-IP with anti-FLAG, probed with anti-ubiquitin and anti-Flag. (**I**) Illustration of USP7 regulating efferocytosis via EPSIN1/LRP1 pathway. CON, control BMDMs; SEN, senescent BMDMs; NC, BMDMs transfected with NC lentivirus; sh*Usp7*, BMDMs transfected with sh*Usp7* lentivirus. Data are presented as means ± SD. $^{*}P < 0.05$, $^{**}P < 0.01$, $^{***}P < 0.001$, $^{****}P < 0.0001$.

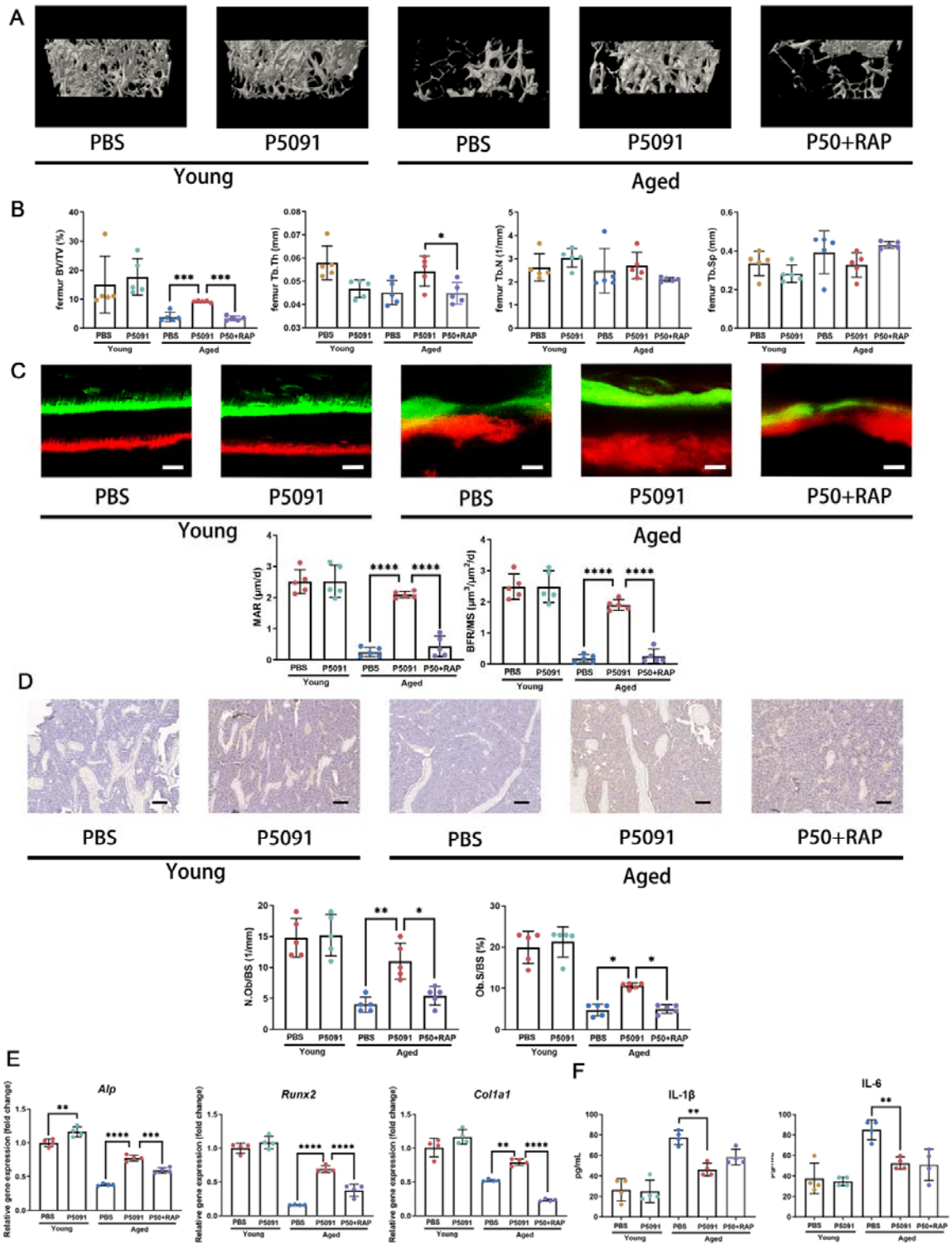

Fig. 6. **P5091 promoted osteoporosis in femurs of aged mice (A)** Representative three-dimensional reconstruction images of femoral trabecular bone (**B**) Quantitative MicroCT analysis of femoral trabecular bone, *n*=5. (**C**) Representative images of calcein and Alizarin Red S double-label fluorescence

staining of femurs followed by quantitative analysis of MAR (mineralization apposition rate) and BFR/MS (bone formation rate per bone surface), *n*=5, scale bar, 20μM. (**D**) Representative images of immunohistochemical staining for ALP followed by quantitative analysis of N.Ob/BS (number of osteoblast per bone surface) and Ob.S/BS (osteoblast surface per bone surface), *n*=5, scale bar, 100μM. (**E**) qPCR results of osteogenic markers in femurs from different groups of mice, *n*=5. (**F**) SASP marker, serum IL-1β and IL-6 analyzed by ELISA, *n*=5. PBS, phosphate buffer saline; RAP, receptor associated protein. Data are presented as means ± SD. *$P < 0.05$, **$P < 0.01$, ***$P < 0.001$, ****$P < 0.0001$.

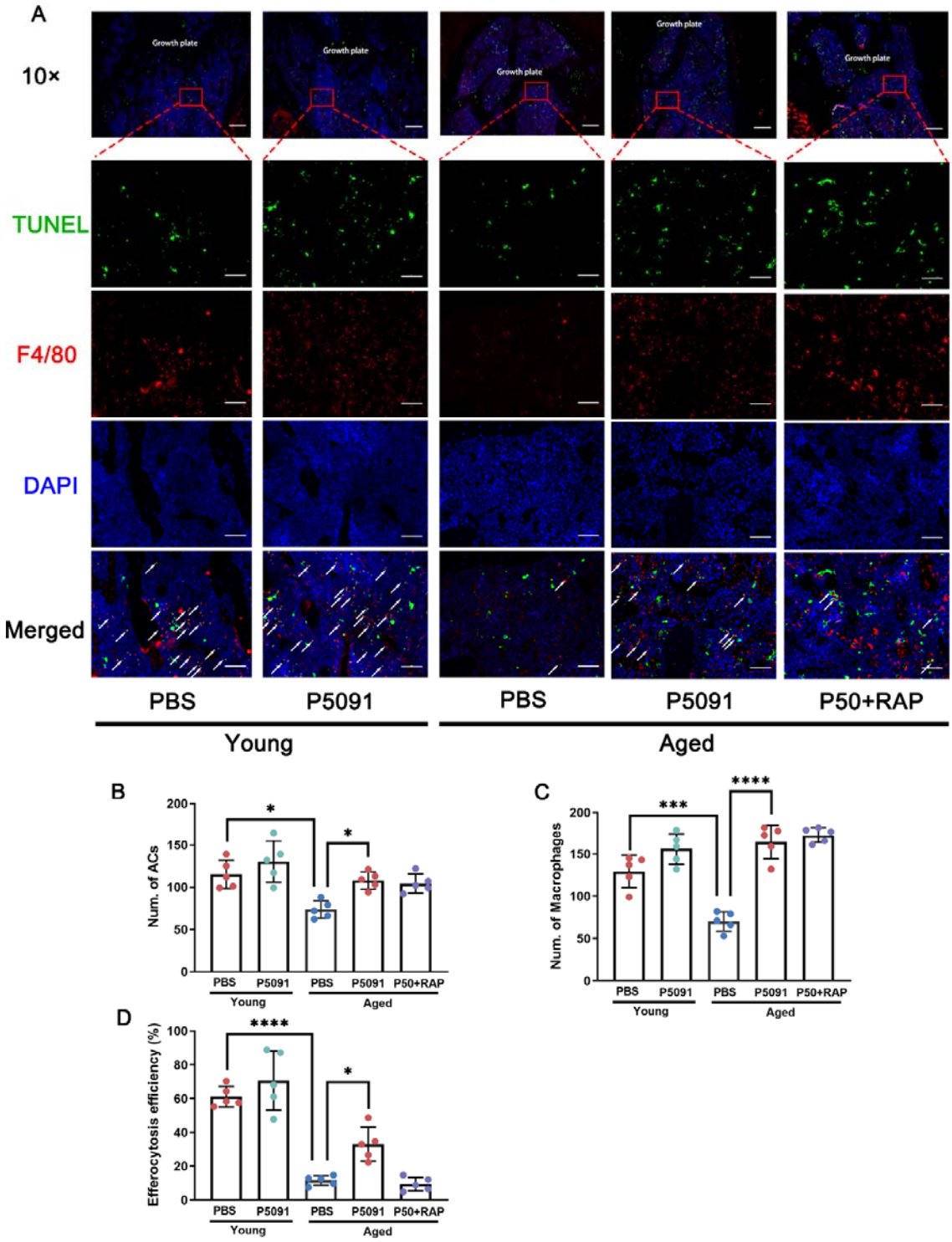

Fig. 7. **P5091 promoted efferocytosis in femurs of aged mice (A**) Representative immunofluorescence images of macrophages and apoptotic cells around the growth plate of femurs, and white arrows indicated the apoptotic cells engulfed by macrophages, followed by quantitative analysis of (**B**) number of apoptotic cells,

(**C**) number of macrophages, (**D**) number of apoptotic cells engulfed by macrophages (efferocytosis efficiency), n=5, scale bar, 40μM. PBS, phosphate buffer saline; RAP, receptor associated protein; ACs, apoptotic cells. Data are presented as means ± SD. *$P < 0.05$, **$P < 0.01$, ***$P < 0.001$, ****$P < 0.0001$.